遠東學報第三十八卷第二期目錄

感知無線隨意網路之適應性合作頻譜感測媒介存取協定

Adaptive Cooperative Spectrum Sensing MAC Protocol for Cognitive Radio Ad Hoc Networks

吳建民　南華大學資訊工程系教授

摘　　要

次要使用者（SU）可以在感知無線隨意網路（CRAHN）中機會式的利用主要使用者（PU）的空閒頻譜，並藉此獲得空閒頻譜建立通訊。然而要達成此目標，必需藉由媒介存取控制（MAC）協定來防止SU和PU之間可能發生的碰撞。本論文提出了一種適用於多跳點和多重通道CRAHN的適應性合作頻譜感測MAC協定（ACMAC）。所提出的ACMAC機制，可以透過MAC協定實現頻譜感測，並藉由合作式的頻譜感測在不須經由其他的控制訊框交換即可得知感測機率。再者，ACMAC可以依據系統負載流適應性的調整競爭視窗長度。因此ACMAC可減少節點能量消耗和資料傳遞延遲，且可提高系統輸出量和通道的重複使用率。本論文也將ACMAC與其他MAC協議進行比較，證明ACMAC在系統效能有更好的表現。

關鍵詞：感知無線隨意網路、媒介存取控制、合作式頻譜感測、多重通道

Chien-Min Wu, Professor, Depart. of Computer Science and Information Engineering, Nanhua University

Abstract

Secondary users (SUs) can opportunistically exploit the idle spectrum of primary users (PUs) in cognitive radio ad hoc networks (CRAHNs). A medium access control (MAC) protocol is needed to prevent collisions between SUs and PUs that may occur while SUs search for licensed and idle channels. In this paper, an adaptive cooperative spectrum sensing MAC protocol (ACMAC) for multihop and multichannel CRAHNs is proposed. With the proposed protocol, sensing probability detection is possible with cooperative spectrum sensing, which is achieved by the exchanging of MAC protocol control frames, without the need for additional sensing control frames. ACMAC is also designed to adaptively adjust the contention window frame length according to the load traffic. Because the ACMAC protocol is both cooperative spectrum sensing and load adaptive, energy consumption and MAC delay are reduced, with increased throughput and channel spatial reuse. We also develop a Markov chain model to characterize the performance of our proposed ACMAC protocol for a saturated network. The Markov chain is also characterized by initial-state probabilities and a state-transition probability matrix. We compare ACMAC with other MAC protocols and show that ACMAC achieves higher performance.

Keywords: cognitive radio ad hoc networks (CRAHNs), medium access control (MAC), cooperative sensing, multichannel

I. Introduction

Regulated spectrum assignment policies for wireless networks are fixed. According to the U.S. Federal Communications Commission, approximately 15 % to 85 % of all activity occurs on fixed spectra. Therefore, the variation in utilized range is high. In addition, spectrum is a limited resource, and using it efficiently is a serious challenge. In order to overcome this challenge, an opportunistic scheme to access spectrum in wireless networks has been proposed as a new communication technology. This new communication mechanism is called a cognitive radio network (CRN) [1].

The idle spectrum of primary users (PUs) can be used opportunistically by secondary users (SUs) in CRNs. Spectrum is divided into many channels in cognitive radio ad hoc networks (CRAHNs). In multichannel CRAHNs, SUs can use the licensed channels of PUs as long as no interference exists among PUs and SUs.

SUs can use the idle licensed PUs channels by sensing the RF environment. Spectrum sensing has two important objects. First, the SU cannot create harmful interference with PUs. Second, SUs can exploit the spectrum holes by efficiently identifying idled spectra. Throughput and quality-of-service (QoS) are achieved by efficiently sensing PUs' channels [2].

Spectrum sensing has two metrics: the probability of false alarm, whereby the SU declares that the PU channel is occupied even though it is actually free; and the probability of misdetection, whereby the SU declares that the PU channel is free even though the spectrum is actually occupied. Misdetections cause interference with PUs and false alarms will decrease channel efficiency [3-6].

Following applications are examples of practical applications for CRNs. The application of CRNs to emergency and public safety communications is achieved by utilizing white space. The executing dynamic spectrum access of potential of CRNs is realized. The military action such as chemical and nuclear attack detection are implemented by the technique of CRNs [7].

While utilizing the spectrum opportunistically in CRNs, medium access control (MAC) protocols can manage interference with PUs, and coordinate spectrum access among SUs. IEEE 802.11 is a widely used single-channel MAC protocol standard. System performance decreases rapidly as the number of SUs increases, owing to increases in contentions and collisions that occur among SUs while using the single-channel architecture of IEEE 802.11 [8].

Utilizing a multichannel scheme is one means of reducing contention and collision among SUs [9]. With the current state of wireless network technology, one SU is allowed to access multiple channels at one time [10].

Therefore, the load adaptive and cooperative spectrum sensing MAC protocol is proposed for work with multihop and multichannel CRAHNs.

The main contributions of the proposed ACMAC protocol are as follows:

1. It is designed for use with multihop and multichannel CRAHNs.
2. Cooperative sensing is achieved by exchanging MAC control frames, and it does need not additional sensing negotiations among SUs.
3. It can adjust the frame length of the contention window adaptively according to actual traffic.
4. It can reduce collisions caused by the hidden terminal problem and increase system throughput by overcoming the exposed terminal problem.

The remainder of this paper is organized as follows. The related work is introduced in Section 2. The system model is introduced in Section 3. The proposed ACMAC protocol are discussed in Section 4. The performance evaluation of multichannel CRAHNs is evaluated in Section 5. The simulation results are discussed in Section 6. Finally, concluding remarks are offered in Section 7.

II. Related Works

A modeling and analytical delay analysis for a multichannel CRN was proposed in [11]. The authors showed that a buffering MAC protocol outperforms a switching MAC protocol. This is because of the delay bottleneck for both protocols, owing to the time required to successfully access the control channel, which occurred more frequently in the switching MAC protocol.

In [12], the authors proposed a preassigned time slot contention free MAC protocol for cooperative spectrum sensing in CRNs. Each SU collects spectrum sensing data and sends that data to the fusion center based on the contention free scheme. However, the preassigned time slot in the spectrum sensing phase will increase the latency of packet transmission.

In [13], the authors proposed a priority-based reservation MAC protocol in slotted single hop multichannel CRNs. A common control channel does not interfere with the PU and is used for SUs to exchange control packets. The control packets include the priority information of accessing PU channels. However, the priority-based reservation MAC protocol is not suitable for multihop CRNs.

In [14], the authors proposed a novel MAC protocol for cognitive radio sensor networks (CRSNs) by selecting a robust PU idle channel. When a PU has the highest idle time as compared to other PU channels, it will be selected as a robust channel. However, a PU with a higher idle time will have a higher interference probability than other PU channels. In addition, a PU with a higher idle time will have a higher number of SUs to access this idle PU channel and will thus increase the collision probability of SUs.

In [15], the authors designed and modeled a performance analysis based on an IEEE 802.11 DCF multichannel MAC protocol for wireless networks. A Markov chain model for CRN was used to model the relations among SUs and PUs. The authors showed that the system throughput and delay are dependent on the number of SUs, the number of PU channels, and the availability of PU channels. Each SU has two transceivers. One is for the control channel to exchange control packets, and the other is for the data channel to transmit data. These two transceivers can work simultaneously.

The primary motivation for almost all previous MAC protocols is to closely monitor throughput, owing to the characteristics of CRAHNs. However, there are other problems of great urgency for CRAHNs, including rate-adaptation, end-to-end propagation delay, and system energy consumption. In addition, there are novel application fields in which CRAHNs can be promoted and developed, including emergency response and public safety [16]. Therefore, a distributed multichannel MAC protocol is needed for the above requirements.

To solve the problems described above, we designed a adaptive cooperative spectrum sensing MAC (ACMAC) protocol to achieve energy-efficiency and low MAC delay. ACMAC can efficiently use available the PU spectrum owing to the use of cooperative sensing and a load adaptive contention window. The PU spectrum is used periodically, with many quiet periods. Therefore, the idle spectrum of PUs can be used by SUs. PUs should not experience performance degradation due to spectrum borrowing by SUs.

In [17], the author proposed real-time scheduling for CRAHNs. Some cellular cognitive base stations are present in CRAHNs. Dynamic channel assignments are determined based on arrival traffic and channel scheduling. Real-time channel assignments are determined based on the past channel allocation status and future traffic conditions of SUs.

In [18], the authors proposed a contention-based distributed MAC (CBMAC) to manage SU channel access in a single-hop cognitive radio ad hoc network (CRAHN). The available data channels of PUs in

CBMAC are utilized by SUs under a contention-based scheme. SUs in CBMAC can reserve idle channels for many periods in order to increase channel utilization. The contention window cycle size of the CBMAC protocol was suitably chosen to keep the interference within a tolerable range.

The number of SUs that win the contention will determine the number of data slots for CBMAC. An SU can easily obtain the number of winners by using the received ACK control frame in the contention window; however, this cannot be achieved in multihop and multichannel CRAHNs. In addition, the optimal number of RTS contention windows in CBMAC cannot be adapted according to real system traffic.

In the proposed ACMAC, each SU adds the sensing outcomes to the MAC protocol control frames. Cooperative sensing is achieved by exchanging MAC protocol control frames. ACMAC also adaptively adjusts the contention window frame length according to actual system traffic. Thus, the average beacon interval in ACMAC is smaller than that in CBMAC, in which the RTS contention window is fixed in advance according to the number of SUs. Additionally, ACMAC keeps interference caused by PUs within a tolerable range, similar to CBMAC.

III. System Model

In this section, we discuss the network model in multichannel CRAHNs. The concepts of IEEE 802.11 PSM are used in ACMAC. Here, there are $n + 1$ non-overlapping channels of the same bandwidth in the proposed ACMAC protocol. And, the number of licensed data channels is n plus one common control channel (CCC). In addition, the licensed channels are known by all the SUs in advance and each SU has two half-duplex transceivers.

A common control channel (CCC) is very suitable for CRAHNs. Several research groups found that a dedicated CCC can be a reliable means of exchanging control information [19]. These studies show that CCCs can be effectively used in CRAHNs. Therefore, we consider the limitations of CCCs when we employ throughput as a metric.

In our proposed ACMAC protocol, two transceivers are installed in each SU. One is responsible for interchanging control messages in the control channel. The other is used by the data channel to transmit data. The control frames are exchanged with other SUs on the control channel, and the SU obtains rights to access the data channels. The data channels are dynamically switched by the data transceiver.

In [11], the authors proposed two MAC protocols: one for buffering and another for switching. In addition, the authors in [11] observed that when using a time-slotted access scheme for the control channel, the buffering MAC protocol outperforms the switching protocol. Therefore, we use the buffering MAC protocol in our ACMAC protocol, because it generally outperforms the switching MAC protocol.

Energy detection measures the energy of a received signal based on the predefined bandwidth and time interval. When the measured energy is greater than the threshold, then the signal is present; otherwise, the signal is absent. Energy detection can be implemented simply and at a low cost under no channel gains and other parameter estimates [20-22].

IV. ACMAC Protocol

In this section, we discuss how ACMAC enables spectrum sharing in multichannel CRAHNs. ACMAC significantly improves throughput and channel spatial reuse by reducing energy consumption and MAC contention delay. ACMAC can alleviate SUs' interference with PUs and reduce collisions among SUs.

1. ACMAC Protocol in Multichannel CRAHNs

In our proposed ACMAC protocol, the beacon

interval is created by dividing the time and spectrum access opportunistically. Each beacon interval has two phases: one involves a sensing window and the other involves a contention window. Each SU senses all the PU channels at the beginning of the beacon interval. Further, each SU records sensing information, including idle PU channels.

Fig 1 shows an ACMAC protocol control channel for a multichannel CRAHN. Next, we will describe the two window phases of ACMAC in detail.

・Sensing window phase. The sensing success probability will decide whether a licensed channel is sensed or not. While the sensing success probability is larger than a threshold, SUs will sense this licensed channel. The sensing success probability is calculated according to the previous three outcomes.

・Contention window phase. There are three control messages that are included in this phase. Those control messages are request-to-send (RTS), clear-to-send (CTS), and reservation channel assignment (RCA). Initially, all frame lengths of RTS/CTS/RCA in the contention window are the same. Further, the frame lengths of RTS/CTS/RCA are adjusted according to actual traffic. new is for when a new node wants to $JOIN$ this network.
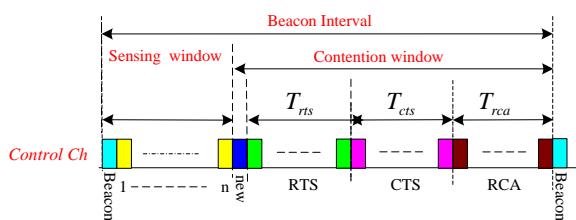

Fig 1 ACMAC control channel in CRAHN.

In Fig 1, T_{rts} denotes the frame length of the RTS field, T_{cts} denotes the frame length of the CTS field, and T_{rca} denotes the frame length of the RCA field. Here, the frame lengths of T_{rts}, T_{cts}, and T_{rca} are all the same.

2. Contention Window Phase

If an SU wants to obtain an idle PU data channel

in a multichannel CRAHN, it must perform those three control messages completely and sequentially. Descriptions for the control messages will be introduced in detail.

・Beacon: Uses IEEE 802.11 TSF.

・INT: INT contains the following fields: CH_{id}, SU_{snd}, and PU_{snd}. CH_{id} denotes the channel interfering with the PU, SU_{snd} denotes the SUs that sent the interrupt message, and PU_{snd} denotes the PU experiencing interference.

・RTS: The initial field in the contention window, from which an SU requests a packet to create a connection. The one-hop neighbors of the SU sender obtain the frame length information and the assigned channel status of all its neighbors in the contention region. Among the fields FL_{snd}, CH_{id1}, CH_{id2}, CH_{id3}, SU_{snd}, SU_{rcv}, $Nbr_{snd1}, \cdots, Nbr_{sndn}$, and $PU_{snd1}, \cdots, PU_{sndn}$, FL_{snd} denotes the frame length of node snd, and CH_{id1}, CH_{id2}, and CH_{id3} have higher priority in the SU sender status. $Nbr_{snd1}, \cdots, Nbr_{sndn}$ denotes the IDs of the neighbors of SU_{snd}. $PU_{snd1}, \cdots, PU_{sndn}$ denotes the sensing outcomes. SU_{snd} and SU_{rcv} denote the SU sender and SU receiver of SU, respectively.

・CTS: The second field in the contention window, to which an SU applies a received RTS control frame. The one-hop neighbors of the SU receiver obtain the frame length information and the assigned channel status of all its neighbors in the contention region. The fields FL_{rcv}, CH_{id}, SU_{snd}, SU_{rcv}, $Nbr_{rcv1}, \cdots, Nbr_{rcvn}$, and $PU_{rcv1}, \cdots, PU_{rcvn}$ are added to the CTS fields of IEEE 802.11. FL_{rcv} denotes the frame length of node rcv. CH_{id} denotes the selected channel from the channel field of the RTS packet. $Nbr_{rcv1}, \cdots, Nbr_{rcvn}$ denotes the one-hop neighbors of the SU_{rcv}. $PU_{rcv1}, \cdots, PU_{rcvn}$ denotes the sensing outcomes.

- RCA: An SU sender receives a CTS control frame and sends a control frame to its neighbors to confirm the beacon interval frame length and assigned data channel information. An RCA contains the fields FL_{snd}, CH_{id}, SU_{snd}, and SU_{rcv}. CH_{id} denotes the coordinating channel that was agreed upon by the SU sender and SU receiver.

  ACK: Contains the fields CH_{id}, SU_{snd}, and SU_{rcv}.

V. Performance Evaluation for the Multichannel CRAHNs

In this section, we present a detailed system performance evaluation of the proposed ACMAC protocol.

1. Channel Spatial Reuse

Assume a CRAHN has n licensed channels that are numbered 1 to n, and M SUs. If SU_i gets licensed channel j, then $CH_j(i)$ is set to 1. Otherwise, $CH_j(i)$ is set to 0. If at least one SU gets channel i, then CH_j is set to 1. Otherwise, CH_j is set to 0.

While one channel can be used by multiple SUs at the same time, we called it channel spatial reuse, which is denoted by ε.

$$\varepsilon = \sum_{k=1}^{Cycle} \frac{\sum_{j=1;Cycle=k}^{n} \sum_{i=1}^{M} CH_j(i)}{\sum_{j=1;Cycle=k}^{n} CH_j} \tag{1}$$

where $Cycle$ is the total number of beacon intervals in the simulation process.

2. Throughput Under Contention Window Size

In [23], the author derived a performance analysis of IEEE 802.11. The saturation throughput of licensed channels is analyzed in [24].

Because the dynamic contention window size for ACMAC and fixed contention window size for CBMAC has different frame length. The throughput per contention window size for this CRAHN due to the simulation ending is defined as ζ, as follows:

$$\zeta = \frac{\varepsilon R_{data} T_{succ} E[CH_{usable}]}{((n-1)R_{data} + R_{ctrl})E[T]} \tag{2}$$

where ε represents the average channel spatial reuse, R_{data} represents data rate for a licensed channel, R_{ctrl} represents the data rate for a control channel, $E[CH_{usable}]$ is the average number of idled channels, T_{succ} is the average transmission time for a successful connection, and the average number of contention slots for the successful handshakes of $RTS/CTS/RCA$ in ACMAC is denoted by $E[T]$ [23, 24]

3. Energy Consumption in MAC Contention

Energy consumption computations will consider three cases: energy consumed while idling, energy consumed during a successful transmission, and energy consumed during a collision [25].

Here, we focus on the energy consumption in MAC contention among SUs. In our proposed ACMAC, E_{succ} and E_{coll} denote the energy consumption for successful and collision MAC contention, respectively. In addition, power on for all SUs are assumed.

- Let $e_{succ}(k)$ denote the k th hop energy consumption of a successful transmission in ACMAC for multichannel CRAHNs. The power consumed while transmitting and receiving RTS, CTS, and RCA are represented by PW_{rts}, PW_{cts}, and PW_{rca}, respectively. The transmission and receiving times for RTS, CTS, and RCA are represent by T_{rts}, T_{cts}, and T_{rca}, respectively. Thus, e_{succ} is computed as follows.

$$e_{succ}(k) = T_{rts}PW_{rts} + T_{cts}PW_{cts} + T_{rca}PW_{rca} \tag{3}$$

- Let $e_{coll}^i(k)$ denote the k th hop energy consumption for the j th trial in a collision MAC contention in ACMAC for multichannel CRAHNs. The energy consumption due to collision transmission will occur in the RTS field of the contention window. Hence, $e_{coll}^i(k)$ is given as follows.

$$e^j_{coll}(k) - T_{rts}PW_{rts} \qquad (4)$$

$$E[E_{consum}] = \frac{\sum_{i=1}^{C_{succ}} \sum_{k=1}^{hop_i} (\sum_{j=1,conn=i}^{n_{trial}} e^j_{coll}(k) + e_{succ}(k))}{\sum_{i=1}^{C_{succ}} hop_i} \qquad (5)$$

where C_{succ} denotes the total number of successful connections, n_{trial} is the sending times for RTS in the MAC contention window before RTS/CTS/RCA handshaking is successful, and hop_i represents the number of hops of the SU source node to the SU destination node for ith connection.

4. MAC Delay Per Hop in Contention Window

Average MAC delay per hop is denoted by $E[T_{delay}]$. The MAC delay per connection is defined as the average time elapsed between the generation of a frame and its successful and complete reception. In the buffering MAC protocol, the MAC delay per connection is the sum of the MAC delays of all occupied channels occurring before a packet is entirely transmitted. The MAC delay for each occupied channel is the sum of the sensing mini-slot window and the successful handshakes of $RTS/CTS/RCA$ in the contention window. Let $t^j_{delay}(k)$ denote the kth hop contention delay for the jth trial for a connection in a MAC contention in ACMAC for multichannel CRAHNs.

$$E[T_{delay}] = \frac{\sum_{i=1}^{C_{succ}} \sum_{k=1}^{hop_i} \sum_{j=1,conn=i}^{n_{trial}} t^j_{delay}(k)}{\sum_{i=1}^{C_{succ}} hop_i} \qquad (6)$$

where C_{succ} denotes the total number of successful connections.

VI. Simulation Results

In this section, we will present the simulation results for our proposed ACMAC. We implemented our simulation with event-driven programming and used the C programming language as the simulation tool. The main difference between ACMAC and CBMAC was the frame length of the contention windows. In CBMAC, the frame length for each field of the contention window is determined by contending nodes. However, CBMAC is not load adaptive in that it cannot adjust the contention window size according to actual traffic. In ACMAC, the contention window size is load adaptive and invokes cooperative sensing. Moreover, it can adjust dynamically. Therefore, we compared ACMAC's performance with the CBMAC scheme. The transmission rate of each data channel is 1 $Mbps$. The control frames consumed 1.675 and 1.425 W of power when transmitting and receiving, respectively. CBMAC-4, CBMAC-8, and CBMAC-16 denote that frame lengths are fixed at 4, 8, and 16 for each RTS/CTS/RCA field in CBMAC, respectively.

PUs alternate between the "PU ON" and "PU OFF" states. The "PU ON" state indicates that a PU is busy on a channel, while the "PU OFF" state indicates that a PU is idle on a channel. We assume that all SUs have fixed locations — this eliminates the effects of broken routes caused by mobility.

In the simulation, we create 10 different topologies using 10 different seeds. The simulation results represent the average of the simulation results for each seed. The topology is divided into 100 areas in order to create a uniform distribution map. We place four SUs in each region randomly. Thus, each SU will have roughly the same average number of neighbors. The number of new arriving connections per second is called the arrival rate. The number of terminated connections is called the departure rate. The average lifetime for a connection is the inverse of the departure rate. If the number of PUs in the PU ON state is 2, it means that the maximum number of simultaneously active PUs is 1 or 2. Because the frame length of the contention window can differ, the number of beacon intervals for ACMAC, CBMAC-4, CBMAC-8, and CBMAC-16 can also differ. Table 1 shows the parameters of our proposed CBMAC multichannel MAC protocol in CRAHNs.

Table 1 Parameters of our proposed CBMAC scheme

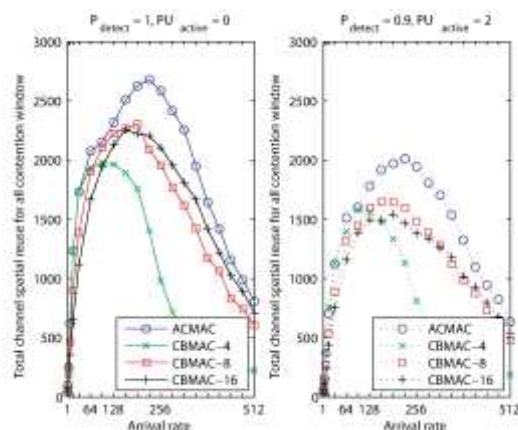| Simulation time	10000 s
Transmission rate	1 Mbps
Power consumption for transmitting	1.675 W
Power consumption for receiving	1.425 W
Frame length	4, 8, 16
Number of active PUs	0, 1, 2
Number of SUs	400

Fig 2 Comparison of total channel spatial reuse in ACMAC and CBMAC versus arrival rate in a multichannel CRAHN

η represents the channel spatial reuse of one beacon interval. The channel spatial reuse is defined as the average number of times that a channel is being used simultaneously. Therefore, η is different in each contention window. Fig 2 shows the summation of η for all beacon intervals in the simulation processes of ACMAC and CBMAC versus the arrival rate in a multichannel CRAHN. For ACMAC, the total channel spatial reuse is higher than in the CBMAC scheme; this is because ACMAC employs cooperative sensing and load adaptive concepts to adjust the contention window size.

From Fig 2, we know that the system achieved saturation when the arrival rate = 192, and that ACMAC produced the highest channel spatial reuse. When the arrival rate exceeded 192, the total channel reuse of ACMAC diminished. We observed that the highest total channel spatial reuse in ACMAC is 2681 (i.e., sensing probability of detection = 1 and PU active = 0). For CBMAC-4, CBMAC-8, and CBMAC-16, the highest total channel spatial reuse in CBMAC-8 is 2256 under arrival rate 192 (i.e., sensing probability of detection = 1 and PU active = 0). The channel spatial reuse of ACMAC improved by as much as 15.8 % compared to CBMAC-8. For ACMAC, channel spatial reuse decreased as PU sensing errors increased. CBMAC-4, CBMAC-8, and CBMAC-16 have lower total channel spatial reuse for all contention windows when sensing probability of detection is 0.9 and PU active is 2.

Fig 3 shows the throughput per contention window size index ζ of channels in ACMAC and CBMAC versus the arrival rate in a multichannel CRAHN. We observed that the highest throughput per contention window size in ACMAC is 5988 under arrival rate = 256 (i.e., sensing probability of detection = 1 and PU active = 0). For CBMAC-8, the highest throughput per contention window size is 4915 at arrival rate = 224 (i.e., sensing probability of detection = 1 and PU active = 0). The throughput per contention window size of ACMAC was improved by as much as 17.9 % compared to CBMAC-8. For ACMAC, the throughput per contention window size decreased while PU sensing errors increased. The maximum throughput will be achieved while the arrival rate for each channel increases. CBMAC-4, CBMAC-8, and CBMAC-16 have lower throughput per contention window size when sensing probability of detect is 0.9 and PU active is 2. Because the channel spatial reuse is higher than 1.0. Hence, the maximum throughput per contention window size is also greater than 1.0.
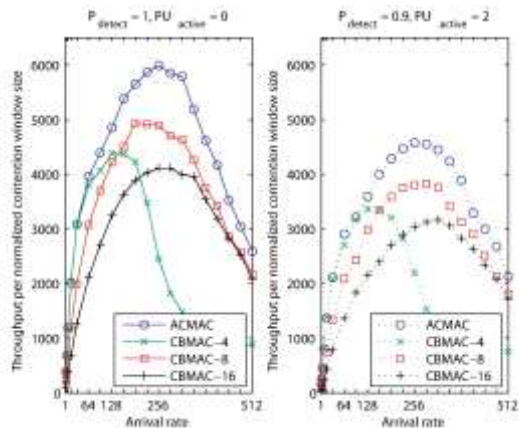
Fig 3 Comparison of throughput per contention window size in ACMAC and CBMAC versus arrival rate on a channel in a multichannel CRAHN
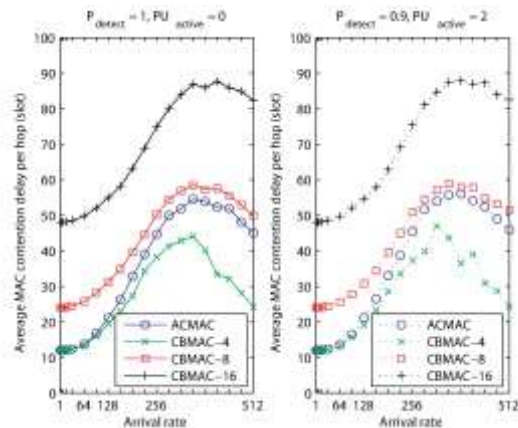

Fig 4 Comparison of average MAC contention delay per hop of SU in ACMAC and CBMAC versus arrival rate in a multichannel CRAHN

Fig 4 shows the average MAC contention delay per hop in ACMAC and CBMAC versus the arrival rate in a multichannel CRAHN. The average MAC contention delay per hop for ACMAC ranges from 12.0 to 54.5 slots (i.e., sensing probability of detection = 1 and PU active = 0) versus different arrival rates. For CBMAC-8, the average MAC contention delay per hop ranges from 24.0 to 58.4 slots (i.e., sensing probability of detection = 1 and PU active = 0) versus different arrival rates. The improvement in average MAC contention delay per hop in ACMAC compared with CBMAC-8 ranges from 6.7 % to 50.0 %. The average MAC contention delay per hop for ACMAC is between those of CBMAC-4 and CBMCA-8. For ACMAC, the average MAC contention delay per hop increased while PU sensing errors increased. CBMAC-8 and CBMAC-16 have higher average MAC contention delay per hop when sensing probability of detection is 0.9 and PU active is 2.

Fig 5 shows the per-hop energy consumption for MAC contentions in ACMAC and CBMAC versus the arrival rate in a multichannel CRAHN. For CBMAC-4, the per-hop energy consumption for MAC contentions is higher than that for ACMAC, CBMAC-8 and CBMAC-16. For ACMAC, the highest per-hop energy consumption for MAC contentions is 13.06 W (i.e., sensing probability of detection = 1 and PU active = 0). For CBMAC-8, the highest per-hop energy consumption for MAC contentions is 13.75 W (i.e., sensing probability of detection = 1 and PU active = 0). There was an 5.0 % improvement in per-hop energy consumption for MAC contentions in ACMAC compared with that CBMAC-8. For ACMAC, the per-hop energy consumption for MAC contentions changed only minimally while PU sensing errors increased. CBMAC-4 and CBMAC-8 have higher per-hop energy consumption for MAC contentions when sensing probability of detection is 0.9 and PU active is 2.

In CBMAC, the frame lengths of each field in all contention windows in the simulation process were the same. In ACMAC, the frame lengths of each field in the contention windows invoked cooperative sensing and were load adaptive according to the actual traffic in the simulation process. Therefore,

ACMAC provided higher total channel spatial reuse for all contention windows and higher throughput per contention window size, and provided reductions in energy consumption and MAC contention delay per hop.
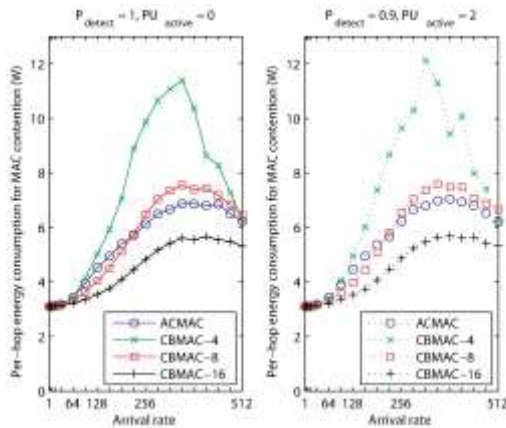

Fig 5 Comparison of per-hop energy consumption for MAC contention of SUs in ACMAC and CBMAC versus arrival rate in a multichannel CRAHN

VII. Conclusion

This paper proposed an adaptive cooperative spectrum sensing MAC contention protocol in multichannel CRAHNs. Cooperative sensing is achieved by the exchanging MAC control frames without the need for additional control frames. Moreover the proposed protocol is load adaptive insofar as the frame length is dynamic. This is achieved by doubling the frame length and halving the frame length according to the actual traffic. We showed that cooperative sensing and a load adaptive contention window length resulted in significant improvements in channel spatial reuse, throughput, delay per hop, and energy efficiency. In ACMAC, per-hop delay reductions were greater than CBMAC-8 and CBMAC-16 because the dynamic contention window saved more idle slots. In ACMAC, per-energy savings were greater than CBMAC-4 and CBMAC-8 because the dynamic contention window saved more idle slots. The proposed ACMAC scheme effectively achieved not only channel spatial reuse but

also improved throughput efficiency. Compared with CBMAC-8, the simulation results showed that reductions in the average MAC contention delay per hop ranged from 6.7 % to 50.0 % and the reduction in per-hop energy consumption for MAC contentions in ACMAC compared was 5.0 % (i.e., sensing probability of detection = 1 and PU active = 0). Additionally, ACMAC saved idle slots, which led to improved channel spatial reuse and throughput. As shown in the simulation results, the throughput per contention window size in ACMAC was improved by as much as 17.9 % compared to CBMAC-8 (i.e., sensing probability of detection = 1 and PU active = 0)

Acknowledgment

References

[1] F. Akyildiz, W. Y. Lee, M. C. Vuran, and S. Mohanty, "NeXt generation/dynamic spectrum access/cognitive radio wireless networks: A survey," Comput. Netw., vol. 50, no. 13, pp. 2127–2159, Sep. 2006.

[2] I. F. Akyildiz, W. Y. Lee, and K.R. Chowdhury, "CRAHNs: cognitive radio ad hoc networks," Ad Hoc Networks, vol. 7, no. 5, pp. 810–836, Sep. 2009.

[3] T. Yucek and H. Arslan, "A survey of spectrum sensing algorithms for cognitive radio applications," IEEE Communications Surveys Tutorials, vol. 11, no. 1, pp. 116-130, Mar. 2009.

[4] M. J. Piran, Q.-V. Pham, S.M. Riazul Islam, S. Cho, B. Bae, D. Y. Suh and Z. Han, "Multimedia communication over cognitive radio networks from QoS/QoE perspective: a

comprehensive survey," Journal of Networks and Computer Applications, vol. 172, pp. 1–44, Dec. 2020.

[5] M. J. Piran, Q.-V. Pham, S.M. Riazul Islam, S. Cho, B. Bae, D. Y. Suh and Z. Han, "The cognitive radio and internet of things, a survey," EJERS, European Journal of Engineering Research and Science, pp. 1–5, Aug. 2020.

[6] A. Nasser, H. A. H. Hassan, J. A. Chaaya, A. Mansour, K.-C. Yao, "Spectrum Sensing for Cognitive Radio: Recent Advances and Future Challenge," Sensors, vol. 21, no. 3, pp. 1–29, Mar. 2021.

[7] M. L. Benitez, "Overview of recent applications of cognitive radio in wireless communication systems," Handbook of Cognitive Radio, Springer, pp. 1–32, Sep. 2018.

[8] S. M. Kamruzzaman, "An energy efficient multichannel MAC protocol for cognitive radio ad hoc networks," International Journal of Communication Networks and Information Security, vol. 2, no. 2, pp. 112–119, Aug. 2010.

[9] R. Maheshwari, H. Gupta, S. R. Das, "Multichannel MAC protocols for wireless networks," Proc. SECON, Reston, VA, USA, Sept. 2006, pp. 393–401.

[10] H. B. Salameh, M. Krunz, O. Younis, "MAC protocol for opportunistic cognitive radio networks with soft guarantees," IEEE Trans. Mobile Comput., vol. 8, no. 10, pp. 1339-1352, Oct. 2009.

[11] S. L. Wu, C. Y. Lin, Y. C. Tseng, and J. P. Sheu, "A new multi-channel MAC protocol with on-demand channel assignment for multi-hop mobile ad hoc networks," in Proc. I-SPAN , Dallas, TX, USA, Dec. 2000, pp. 232–237.

[12] J. Jia, Q. Zhang, and X. Shen, "HC-MAC: a hardware-constrained cognitive MAC for efficient spectrum management," IEEE J. Sel. Areas Commun., vol. 7, no. 1, pp. 106–117, Jan. 2008.

[13] Q. Zhao, L. Tong, A. Swami, and Y. Chen, "Decentralized cognitive MAC for opportunistic spectrum access in ad hoc networks: a POMDP framework," IEEE J. Sel. Areas Commun., vol. 25, no. 3, pp. 589–600, Apr. 2007.

[14] B. Hamdaoui and K. G. Shin, "OS-MAC: an efficient MAC protocol for spectrum-agile wireless networks," IEEE Trans. Mobile Comput., vol. 7, no. 8, pp. 915-30, June 2008.

[15] C. Cordeiro and K. Challapali, "C-MAC: a cognitive MAC protocol for multi-channel wireless networks," in Proc. IEEE DySPAN, Dublin, Apr, 2007, pp. 147-157.

[16] H. Su and X. Zhang, "CREAM-MAC: an efficient cognitive radio enabled multi-channel MAC protocol for wireless networks," in Proc. WoWMoM, Newport Beach, CA, June 2008, pp. 1–8.

[17] L. Le and E. Hossain, "OSA-MAC: a MAC protocol for opportunistic spectrum access in cognitive radio networks," in Proc. IEEE WCNC, Las Vegas, NV, Apr. 2008, pp. 1426–1430.

[18] W. S. Jeon, J. A. Han, and D. G. Jeong, "A novel MAC scheme for multichannel cognitive radio ad hoc networks," IEEE Trans. Mobile Comput., vol. 11, no. 6, pp. 922–934, June 2012.

[19] M. Timmers, S. Pollin, A. Dejonghe, L.V. Perre, and F. Catthoor, "A distributed multichannel MAC protocol for multihop cognitive radio networks," IEEE Trans. Veh. Technol., vol. 59, no. 1, pp. 446–459, Aug. 2009.

[20] Y. H. Lee and D. Kim, "Slow hopping based cooperative sensing MAC protocol for cognitive radio networks," Comput. Netw., vol. 62, no. 7, pp. 12–28, Apr. 2014.

[21] B. Wang, K. J. Ray Liu, "Advances in cognitive radio networks: A survey," IEEE J. Sel. Areas Commun., vol. 5, no. 1, pp. 5–23, Nov. 2010.

[22] S. Debroy, S. De, and M. Chatterjee, "Contention based multichannel MAC protocol for distributed cognitive radio networks," IEEE Trans. Mobile Comput., vol. 13, no. 12, pp. 2749-2762, Dec. 2014.

[23] S. Maleki, A. Pandharipande, and G. Leus "Energy-efficient distributed spectrum sensing for cognitive sensor networks," IEEE Sensors Journal, vol. 11, no. 3, pp. 565–573, Mar. 2011.

[24] S. Kumar and D. K. Lobiyal, "Sensing coverage prediction for wireless sensor networks in shadowed and multipath environment," The Scientific World Journal. , vol. 2013, pp. 1–11, Sep. 2013.

[25] F.F. Digham, M.S. Alouini and M.K. Simon "On the energy detection of unknown signals over fading channels," IEEE Trans. On Commun., vol. 55, no. 1, pp. 21–24, Jan. 2007.

具漏感能量回收之高功率因數電源供應器之研究

Study of a High Power Factor Power Supply with Leakage-Inductance Energy Recycling

楊隆生　遠東科技大學電機工程系副教授

楊銘昆　遠東科技大學電機工程系學生

摘　　要

本論文旨在研究具漏感能量回收之高功率因數電源供應器。本電源供應器的前級為交流-直流升壓型轉換器作功率因數修正用，採連續導通模式控制，達到高功率因數及低輸入電流諧波。本電源供應器的後級為直流-直流轉換器，採用單開關整合雙組返馳式轉換器的架構，提供降壓功能及電氣隔離。同時達到變壓器漏感能量回收。論文中對交流-直流升壓型轉換器及雙組直流-直流返馳式轉換器的操作原理及穩態分析均作詳細討論，並進行電腦模擬以驗證本電源供應器的性能。

關鍵詞：功率因數修正、返馳式轉換器、漏感能量回收

Lung-Sheng Yang, Associate Professor, Department of Electrical Engineering, Far East University

Ming-Kun Yang, Undergraduate Student, Department of Electric Engineering, Far East University

Abstract

A high power factor power supply with leakage-inductance energy recycling is studied in this paper. The front stage of the proposed power supply is an AC-DC boost converter. This converter is used for power factor correction. It adopts continuous conduction mode to achieve high power factor and low input current harmonic. The rear stage of the proposed power supply is a DC-DC converter. This converter integrates two flyback converter using a single switch for step-down voltage conversion and electrical isolation. Also, the leakage-inductance energy can be recycled. In this paper, the operation principles and steady-state analyses of the AC-DC boost converter and the two DC-DC flyback converter are discussed in detail. Finally, the computer simulations are performed to verify the performance of the proposed power supply.

Keywords: power factor correction, flyback converter, leakage-inductance energy recycling

一、前　言

　　現今各種電子產品皆需要不同的直流電源，因此需要將交流電源轉換成直流電源。傳統的橋式交流-直流轉換器可提供直流電源以供使用，這種轉換器的優點為架構簡單及成本低。缺點為體積大、低功率因數、及高輸入電流諧波。因此若干文獻提出不同電路架構，以達到輸入電流為正弦波、低諧波成份、高功率因數、及穩定的直流輸出電壓之特性。此外這些電路架構為高頻式切換，因此轉換器的體積大幅度縮小。切換式電源供應器的前級為交流-直流轉換器作功率因數修正用，如升壓型[1]-[3]、降壓型[4]-[6]、及降-升壓型等[7]-[9]。後級為直流-直流轉換器提供降壓功能，如降壓型[10]-[12]、返馳式[13]-[16]、順向式[17]-[20]、半橋型[21]-[23]、及全橋型等[24]-[26]。

　　傳統返馳式直流-直流電源轉換器具有架構簡單，單開關電路控制較容易，且成本較低等優點，但此電路架構有變壓器漏感能量無法回收的缺點，需額外使用緩震電路，以降低變壓器漏感與切換開關上的寄生電容振盪造成之電壓突波。然而，緩震電路的使用亦伴隨著功率損耗，造成能量的浪費與效率的降低。同時返馳式變壓器漏感與切換開關上的寄生電容振盪造成之電壓突波，使得在電路設計上選用合適的功率開關更為困難，也因上述這些原因，傳統的返馳式電源轉換器多被應用在中低功率(5~150 Watts)。

　　本論文研究「具變壓器漏感能量回收的單開關雙組返馳式電源供應器」，電路架構方塊圖如圖1所示。前級交流-直流轉換器採用連續電流導通模式之升壓型功率因數修正器，達到高功率因數及低輸入電流諧波。後級直流-直流轉換器採單開關整合雙組返馳式轉換器，將變壓器之漏感能量回收以改善轉換效率與電磁干擾，實現高效能電源供應器。
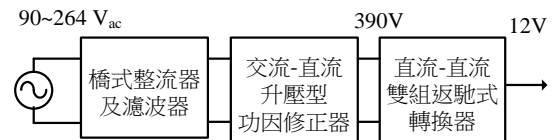
圖 1　本轉換器電路架構
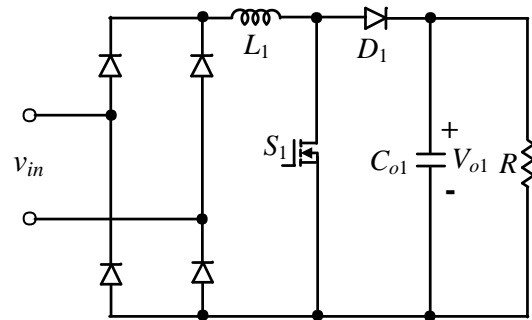
圖 2　交流-直流升壓型功率因數修正器

二、交流-直流升壓型功率因數修正器

　　圖 2 為交流-直流升壓型功率因數修正器之電路架構。採用連續電流導通模式之平均電流控制模式，包含兩個回授控制電路，外部迴路為電壓回授控制，內部迴路為電流回授控制，以完成高功率因數、低輸入電流諧波、及穩定的輸出電壓。

本轉換器於電源正半波時的操作模式如下：

模式 1：切換開關 S_1 導通，電流路徑如圖 3(a)所示。輸入電源 v_{in} 的能量經由橋式整流器及切換開關 S_1，傳送給電感器 L_1。輸出電容器 C_{o1} 將儲存的能量供應給負載 R。此時電感器 L_1 儲存能量，電感電流 i_{L1} 呈現遞增。

模式 2：切換開關 S_1 截止，電流路徑如圖 3(b)所示。輸入電源 v_{in} 與電感器 L_1 串聯將其能量經由橋式整流器及二極體 D_1 傳送給輸出電容器 C_{o1} 及負載 R。此時電感器 L_1 釋放能量，電感電流 i_{L1} 呈現遞減。
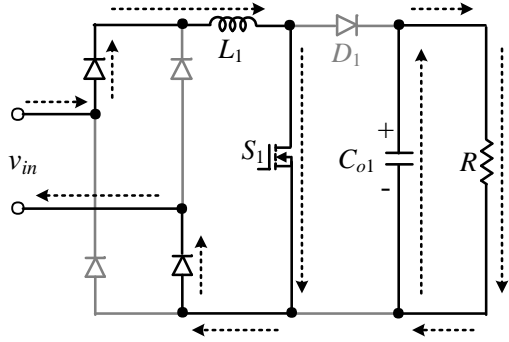
(a)模式 1
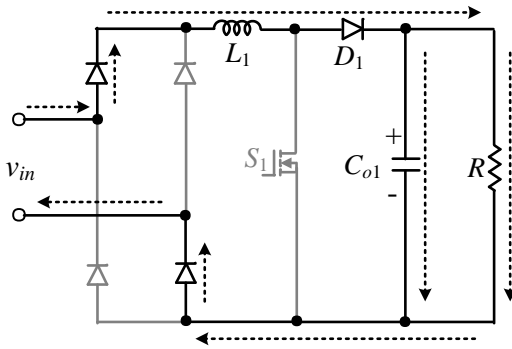
(b)模式 2

圖 3 本轉換器操作於電源正半波時電流路徑圖

三、直流-直流雙組返馳式轉換器

具漏感能量回收功能之單開關直流-直流雙組返馳式轉換器，電路架構如圖 4 所示。兩變壓器 T_1 及 T_2 兼具儲能及變壓之功能，且匝數比及磁化電感均相同。圖 5 為本轉換器之等效電路。當切換開關導通時，兩變壓器 T_1 及 T_2 之磁化電感及一次側漏電感儲存能量。當切換開關截止時，儲存於兩變壓器 T_1 及 T_2 之磁化電感的能量並聯傳送至輸出電容器 C_o 及負載 R。同時，兩變壓器 T_1 及 T_2 之一次側漏電感的能量分別傳送至電容器 C_1 及 C_2，達到兩變壓器 T_1 及 T_2 漏感能量回收的功能以提升轉換效率。本轉換器的優點：

(1)僅使用單一切換開關。

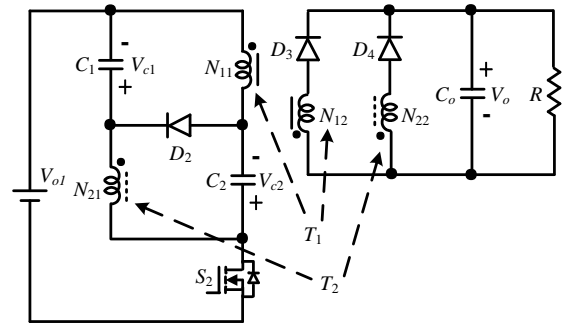(2)變壓器漏感能量可回收，提升轉換效率。
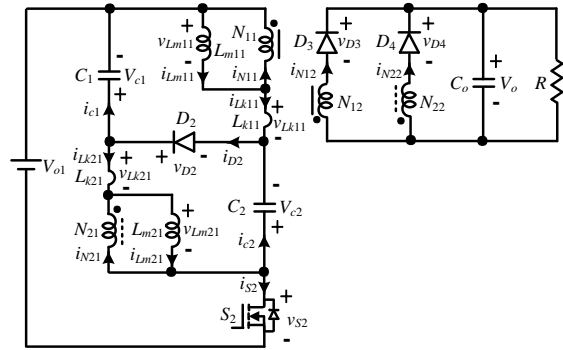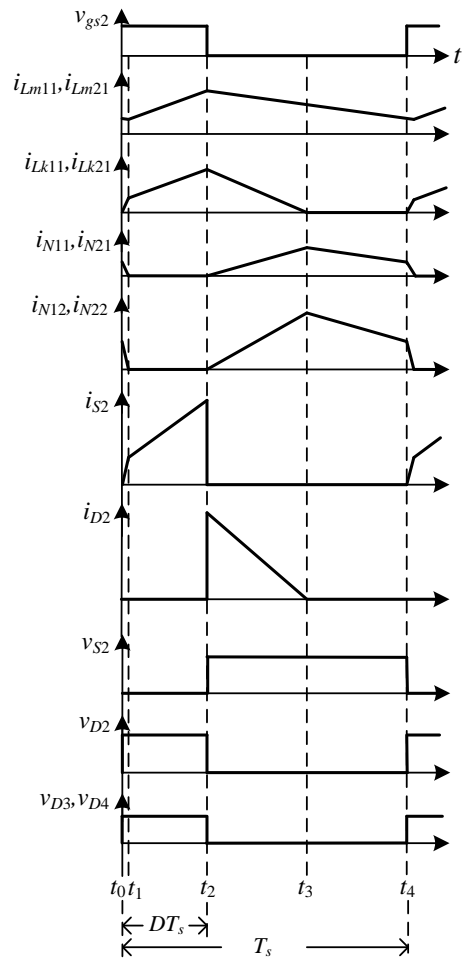
(3)提供電氣隔離功能。

(4)切換開關電壓被箝位，以降低切換開關電壓應力。

圖 4 單開關直流-直流雙組返馳式轉換器

圖 5 本轉換器之等效電路圖

圖 6 本轉換器於單一切換週期之主要波形圖

本轉換器採用脈波寬度調變技術控制切換開關 S_1。圖 6 為本轉換器於單一切換週期之主要波形圖。本轉換器之變壓器 T_1 及 T_2 具有相同匝數,因此

$$L_{m11} = L_{m21} = L_m \qquad (1)$$

$$L_{k11} = L_{k21} = L_k \qquad (2)$$

$$V_{c1} = V_{c2} = V_c \qquad (3)$$

本轉換器之操作模式敘述如下:

模式 1:區間[t_0, t_1],切換開關 S_2 導通,電流路徑如圖 7(a)所示。儲存於兩變壓器之磁化電感 L_{m1}、L_{m2} 及輸出電容器 C_o 的能量並聯釋放給負載 R。電源 V_{o1}、電容器 C_1、磁化電感 L_{m2} 串聯釋放能量給變壓器漏電感 L_{k2}。同樣地,電源 V_{o1}、電容器 C_2、磁化電感 L_{m1} 串聯釋放能量給變壓器漏電感 L_{k1}。因此流經磁化電感的電流 i_{Lm1} 及 i_{Lm2} 呈線性下降,流經漏電感的電流 i_{Lk1} 及 i_{Lk2} 呈線性上升。在 $t = t_1$ 時,磁化電感電流 i_{Lm1} 及 i_{Lm2} 等於漏電感電流 i_{Lk1} 及 i_{Lk2},本操作模式結束。

模式 2:區間[t_1, t_2],切換開關 S_2 持續導通,電流路徑如圖 7(b)所示。電源 V_{o1} 與電容器 C_1 串聯釋放能量給變壓器磁化電感 L_{m2} 及漏電感 L_{k2}。同樣地,電源 V_{o1} 與電容器 C_2 串聯釋放能量給變壓器磁化電感 L_{m1} 及漏電感 L_{k1}。輸出電容器 C_o 則釋放能量給負載 R。因此磁化電感電流 i_{Lm1}、i_{Lm2} 及漏電感電流 i_{Lk1}、i_{Lk2} 呈線性上升。在 $t = t_2$ 時,切換開關 S_2 截止,本操作模式結束。磁化電感電壓方程式為

$$v_{Lm}^{II} = k(V_{in} + V_c) \qquad (4)$$

模式 3:區間[t_2, t_3],切換開關 S_2 截止,電流路徑如圖 7(c)所示。磁化電感 L_{m2} 及漏電感 L_{k2} 串聯釋放能量給電容器 C_2。同樣地,磁化電感 L_{m1} 及漏電感 L_{k1} 串聯釋放能量給

電容器 C_1。因此漏電感 L_{k1} 及 L_{k2} 的能量可分別回收至電容器 C_1 及 C_2。同時,儲存於磁化電感 L_{m1}、L_{m2} 及輸出電容器 C_o 的能量並聯釋放給負載 R。因此磁化電感電流 i_{Lm1}、i_{Lm2} 及漏電感電流 i_{Lk1}、i_{Lk2} 呈線性下降。在 $t = t_3$ 時,漏電感電流 $i_{Lk1} = i_{Lk2} = 0$,即漏電感 L_{k1} 及 L_{k2} 的能量回收完畢,本操作模式結束。
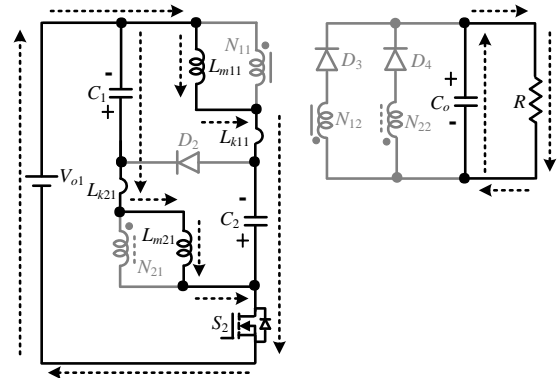
$$v_{Lm}^{III} = -\frac{V_o}{n} \qquad (5)$$

模式 4:區間[t_3, t_4],切換開關 S_2 仍然截止,電流路徑如圖 7(d)所示。儲存於磁化電感 L_{m1} 及 L_{m2} 的能量並聯釋放給輸出電容器 C_o 及負載 R。因此磁化電感電流 i_{Lm1} 及 i_{Lm2} 呈線性下降。本操作模式結束在下一個切換週期開始,切換開關 S_2 導通。
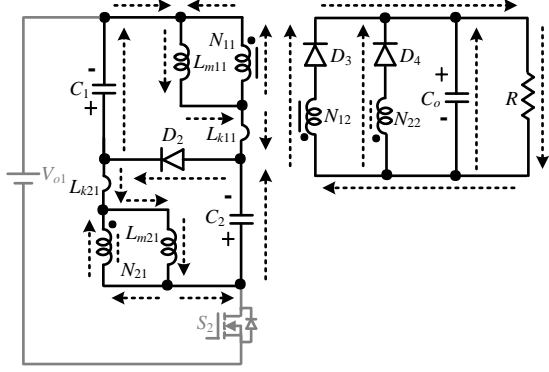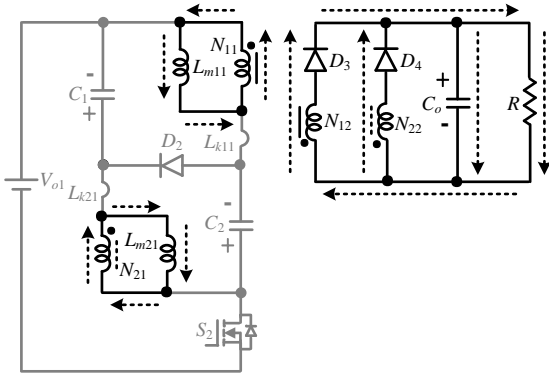
$$v_{Lm}^{IV} = -\frac{V_o}{n} \qquad (6)$$
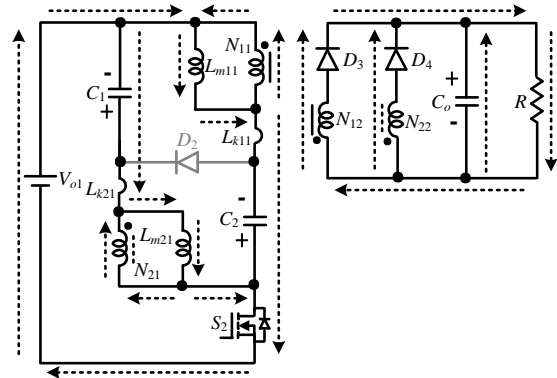
(a) 模式 1

(b) 模式 2

(c) 模式 3

(d) 模式 4

圖 7 本轉換器各操作模式之電流路徑圖

利用磁化電感之伏秒平衡原理知

$$v_{Lm}^{II} D T_s + v_{Lm}^{III}(t_3 - t_2) + v_{Lm}^{IV}(t_4 - t_3) = 0 \qquad (7)$$

將方程式(4)-(6)代入方程式(7)可得

$$kD(V_{in} + V_c) = \frac{V_o}{n}(1 - D) \qquad (8)$$

其中

$$k = \frac{L_m}{L_m + L_k} \qquad (9)$$

$$n = \frac{N_{12}}{N_{11}} = \frac{N_{22}}{N_{21}} \qquad (10)$$

電容器電壓為

$$V_c = \frac{V_o}{n} \qquad (11)$$

忽略變壓器漏電感的影響，$k = 1$。將 $k = 1$ 及方程式(11)代入方程式(8)可得

$$M = \frac{V_o}{V_{in}} = \frac{nD}{1 - 2D} \qquad (12)$$

因此操作限制為責任週期 D 必須小於 0.5。

邊界條件為

$$\tau_{LmB} = \frac{L_{mB} f_s}{R} = \frac{(1-D)^2}{n^2} \qquad (13)$$

功率切換元件之電壓應力

$$V_{S2} = V_{D2} = V_{in} + 2V_c = V_{in} + \frac{2V_o}{n} \qquad (14)$$

$$V_{D3} = V_{D4} = n(V_{in} + V_c) + V_o = nV_{in} + 2V_o \qquad (15)$$

四、電路模擬

本轉換器電氣規格及元件參數如下：

輸入電壓 v_{in} = 90~264 V_{rms}、前級輸出電壓 V_{o1} = 390 V_{DC}、輸出功率 P_o = 360 W、功率因數修正器切換頻率 f_{s1} = 65 kHz、電感器 L_1 = 940 μH、電容器 C_{o1} = 270 μF、輸出電壓 V_o = 12 V_{DC}、雙組返馳式轉換器切換頻率 f_{s2} = 50 kHz、變壓器匝數比 n = 0.1、電容器 $C_1 = C_2$ = 100 μF、C_o = 3300 μF。由上列知電壓增益 M = 0.031。將電壓增益 M = 0.031 及變壓器匝數比 n = 0.1 代入方程式(12)可得責任週期 D = 0.191。將責任週期 D = 0.191 代入方程式(13)可得 τ_{LmB} = 65.45。選定 50%以上負載本轉換器操作在連續導通模式，因此等效電阻 R = 0.8 Ω。所以

$$L_m > L_{mB} = \frac{\tau_{LmB} R}{f_{s2}} = \frac{65.45 \times 0.8}{50k} = 1047.2 \ \mu H$$

因此變壓器磁化電感選擇 $L_{m1} = L_{m2}$ = 1050 μH。使用電腦軟體 PSIM 作模擬。由圖 8 及 9 可看出在輸入電壓為 100 V_{rms} 及 240 V_{rms} 時，輸入電壓及輸入電流幾乎同相位，功率因數趨近於 1。而且輸入電流幾近正弦波，諧波成分相當低。圖 10 為修正電路輸出電壓 V_{o1}、電容器電壓 V_{c1} 及輸出電壓 V_o 之模擬波形，可看出輸出電壓 V_o 被穩定控制在 12 V，及電容器電壓 V_{c1} 約為 V_o/n = 120 V。圖 11 為變壓器漏感電流 i_{Lk1} 及電容器電流 i_{c1} 之模擬波形。在切換開關 S_2 截止時 i_{Lk1} = i_{c1}，表示漏電感 L_{k1} 的能量回收至電容器 C_1。圖 12 為切換開關 S_2 之電壓及電

流模擬波形,電壓約箝位於 $V_{S2} = V_{o1} + 2V_o/n = 630$ V。圖 13 為二極體 D_2 之電壓及電流模擬波形,電壓應力約為 $V_{D2} = V_{o1} + 2V_o/n = 630$ V。圖 14 為二極體 D_3 之電壓及電流模擬波形,電壓應力約為 $V_{D3} = n V_{o1} + 2V_o = 63$ V。
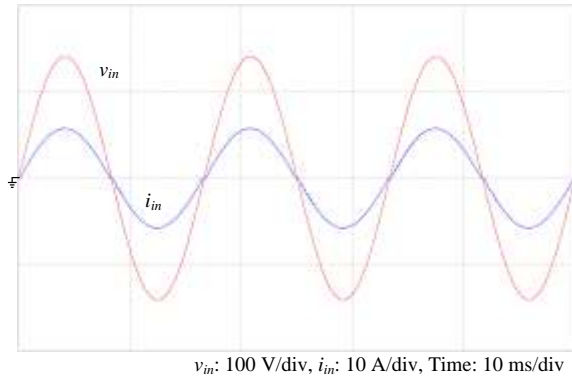

v_{in}: 100 V/div, i_{in}: 10 A/div, Time: 10 ms/div

圖 8 操作於輸入電壓 100V$_{rms}$、修正電路輸出電壓 390 V、輸出電壓 12 V 時,輸入電壓 v_{in} 及輸入電流 i_{in} 之模擬波形

v_{in}: 250 V/div, i_{in}: 5 A/div, Time: 10 ms/div
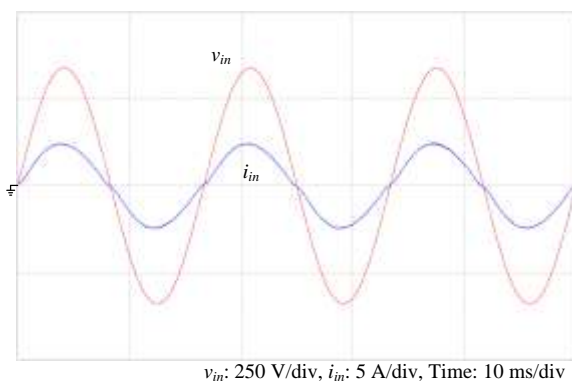
圖 9 操作於輸入電壓 240V$_{rms}$、修正電路輸出電壓 390 V、輸出電壓 12 V 時,輸入電壓 v_{in} 及輸入電流 i_{in} 之模擬波形

V_{o1}, V_{c1}, V_o: 100 V/div, Time: 100 μs/div

圖 10 電壓 V_{o1}、V_{c1}、及 V_o 之模擬波形

i_{Lk1}, i_{c1}: 5 A/div, Time: 20 μs/div
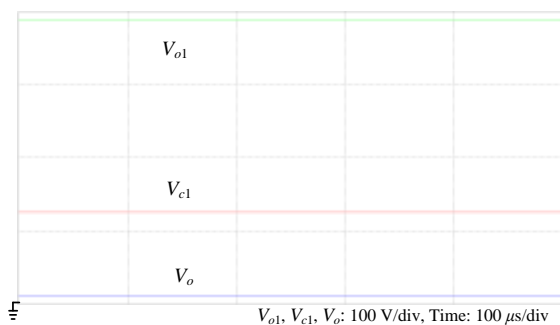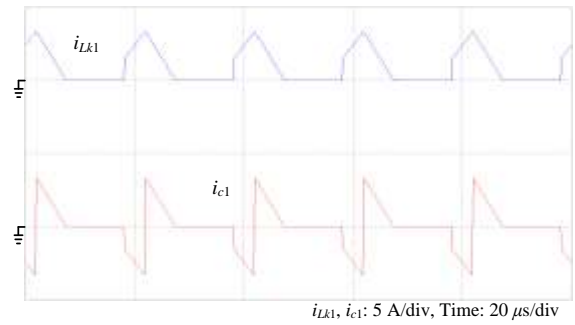
圖 11 變壓器漏感電流 i_{Lk1} 及電容電流 i_{c1} 之模擬波形

v_{s2}: 500 V/div, i_{s2}: 5 A/div, Time: 20 μs/div
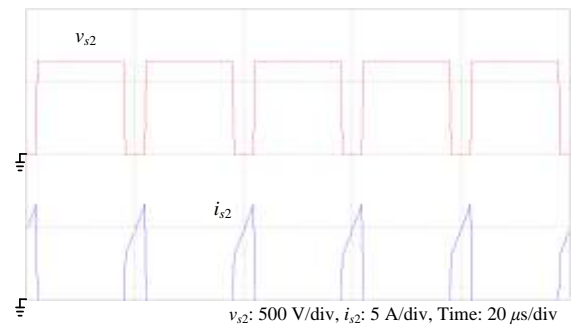
圖 12 切換開關電壓 v_{S2} 及電流 i_{S2} 之模擬波形

v_{D2}: 500 V/div, i_{D2}: 5 A/div, Time: 20 μs/div

圖 13 二極體電壓 v_{D2} 及電流 i_{D2} 之模擬波形

i_{Do1}: 25 A/div, v_{Do1}: 25 V/div, Time: 20 μs/div
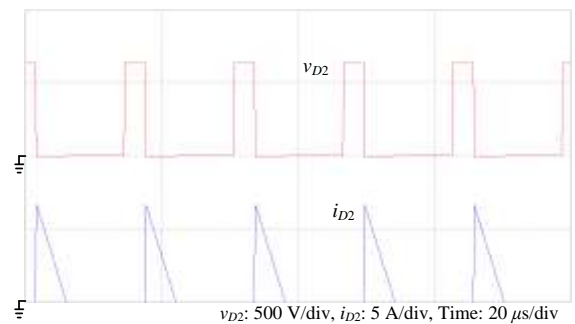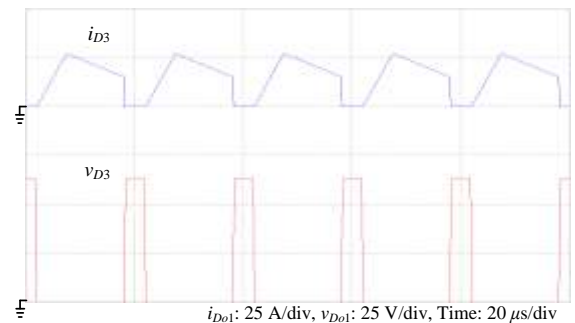
圖 14 二極體電壓 v_{D3} 及電流 i_{D3} 之模擬波形

五、結　論

　　本論文研究一高效能高功率因數電源供應器，本電源供應器之前級為交流-直流升壓型轉換器之功率因數修正電路，採連續導通模式控制，達到高功率因數，並降低電流諧波，提升用電效率。本電源供應器之後級為直流-直流雙組返馳式轉換器，採單開關控制，具變壓器漏感能量回收的功能。由模擬結果，可看出在泛用型輸入電壓(90~264 Vms)下，皆可完成高功率因數、低輸入電流諧波、穩定輸出電壓、及變壓器漏感能量回收的高效能電源供應器。

參考文獻

[1] M. Lee and J. S. Lai, "Unified voltage balancing feedforward for three-level boost PFC converter in discontinuous and critical conduction modes," IEEE Transactions on Circuits and Systems II: Express Briefs, vol. 68, no. 1, pp. 441-445, 2021.

[2] 曾國軒，數位式升壓型功率因數修正器的研製，中華民國104年國立臺北科技大學電機工程系碩士論文。

[3] M. M. Cheng, Z. Liu, Y. Bao, and Z. Zhang, "Continuous conduction mode soft-switching boost converter and its application in power factor correction," Journal of Power Electronics, vol. 16, no. 5, pp. 1689-1697, 2016.

[4] M. Malekanehrad and E. Adib, "Bridgeless buck PFC rectifier with improved power factor," Journal of Power Electronics, vol. 18, no. 2, pp. 323-331, 2018.

[5] M. Malekanehrad and E. Adib, "A novel single-phase buck PFC AC-DC converter with power decoupling capability using an active buffer," IEEE Transactions on Industry Applications, vol. 50, no. 3, pp. 1905-1914, 2014.

[6] V. F. Pires and J. F. Silva, "Single-stage double-buck topologies with high power factor," Journal of Power Electronics, vol. 11, no. 5, pp. 655-661, 2011.

[7] 陳志熒，寬輸出電壓之串接型降壓-升壓功率因數修正器研製，中華民國103年國立虎尾科技大學航空與電子科技研究所碩士論文。

[8] K. M. Siu and C. N. M. Ho, "Manitoba rectifier-bridgeless buck-boost PFC," IEEE Transactions on Power Electronics, vol. 35, no. 1, pp. 403-414, 2020.

[9] I. Abdelsalam, G. P. Adam, D. Holliday, and B. W. Williams, "Single-stage, single-phase, ac-dc buck-boost converter for low-voltage applications," IET Power Electronics, vol. 7, no. 10, pp. 2496-2505, 2014.

[10] 林奕辰，高切換頻率的數位控制直流對直流降壓型轉換器設計，中華民國106年國立臺灣大學電子工程學研究所碩士論文。

[11] C. Zhang, J. Wang, S. Li, B. Wu, and C. Qian, "Robust control for PWM-based DC-DC buck power converters with uncertainty via sampled-data output feedback," IEEE Transactions on Power Electronics, vol. 30, no. 1, pp. 504-515, 2015.

[12] A. E. Aroudi, B. A. M. Trevino, E. V. Idiarte, L. M. Salamero, "Analysis of start-up response in a digitally controlled boost converter with constant power load and mitigation of inrush current problems," IEEE Transactions on Circuits and Systems I: Regular Papers, vol. 67, no. 4, pp. 1276-1285, 2020.

[13] J. Li, F. B. M. V. Horck, B. J. Daniel, and H. J. Bergveld, "A high-switching-frequency flyback converter in resonant mode," IEEE Transactions on Power Electronics, vol. 32, no. 11, pp. 8582-8592, 2017.

[14] J. W. Yang and H. L. Do, "Soft-switching dual-flyback DC-DC converter with improved efficiency and reduced output ripple current," IEEE Transactions on Industrial Electronics, vol.

64, no. 5, pp. 3587-3594, 2017.

[15] 林致緯，準諧振返馳式轉換器之新型控制策略研製，中華民國107年國立虎尾科技大學車輛工程系碩士論文。

[16] H. Dong, X. Xie, and L. Zhang, " A new primary PWM control strategy for CCM synchronous rectification flyback converter," IEEE Transactions on Power Electronics, vol. 35, no. 5, pp. 4457-4461, 2020.

[17] H. Wu and Y. Xing, "Families of forward converters suitable for wide input voltage range applications," IEEE Transactions on Power Electronics, vol. 29, no. 11, pp. 6006-6017, 2014.

[18] E. Chu, J, Bao, H. Xie, and G. Hui, " A zero-voltage and zero-current switching interleaved two-switch forward converter with passive auxiliary resonant circuit," IEEE Transactions on Power Electronics, vol. 35, no. 5, pp. 4859-4876, 2020.

[19] S. J. Chen, S. P. Yang, and M. F. Cho, "Analysis and implementation of an interleaved series input parallel output active clamp forward converter," IET Power Electronics, vol. 6, no. 4, pp. 774-782, 2013.

[20] H. Wu, P. Xu, W. Liu, and Y. Xing, "Series-input interleaved forward converter with a shared switching leg for wide input voltage range applications," IEEE Transactions on Industrial Electronics, vol. 60, no. 11, pp. 5029-5039, 2013.

[21] F. Liu, Z. Wang, Y. Mao, and X. Ruan, "Asymmetrical half-bridge double-input DC/DC converters adopting pulsating voltage source cells for low power applications," IEEE Transactions on Power Electronics, vol. 29, no. 9, pp. 4741-4751, 2014.

[22] X. Yu, K. Jin, and Z. Liu, "Capacitor voltage control strategy for half-bridge three-level DC/DC converter," IEEE Transactions on Power Electronics, vol. 29, no. 6, pp. 1557-1561, 2014.

[23] A. K. Rathore and U. R. Prasanna, "Analysis, design, and experimental results of novel snubberless bidirectional naturally clamped ZCS/ZVS current-fed half-bridge DC/DC converter for fuel cell vehicles," IEEE Transactions on Industrial Electronics, vol. 60, no. 10, pp. 4482-4491, 2013.

[24] G. N. B. Yadav and N. L. Narasamma, "An active soft switched phase-shifted full-bridge DC-DC converter: analysis, modeling, design, and implementation," IEEE Transactions on Power Electronics, vol. 29, no. 9, pp. 4538-4550, 2014.

[25] Y. D. Kim, I. O. Lee, I. H. Cho, and G. W. Moon, "Hybrid dual full-bridge DC-DC converter with reduced circulating current, output filter, and conduction loss of rectifier stage for RF power generator application," IEEE Transactions on Power Electronics, vol. 29, no. 3, pp. 1069-1081, 2014.

[26] S. H. Ryu, D. H. Kim, M. J. Kim, J. S. Kim, and B. K. Lee, "Adjustable frequency-duty-cycle hybrid control strategy for full-bridge series resonant converters in electric vehicle chargers," IEEE Transactions on Industrial Electronics, vol. 61, no. 10, pp. 5354-5362, 2014.